Atomic imaging of nucleation of trimethylaluminum on clean and H_2O functionalized Ge(100) surfaces

Joon Sung Lee,[1,2] Tobin Kaufman-Osborn,[1,2] Wilhelm Melitz,[1,2] Sangyeob Lee,[2] Annelies Delabie,[3] Sonja Sioncke,[3] Matty Caymax,[3] Geoffrey Pourtois,[3] and Andrew C. Kummel[2,a)]

[1]*Materials Science and Engineering Program, University of California, San Diego, 9500 Gilman Drive MC0358, La Jolla, California 92093, USA*
[2]*Department of Chemistry and Biochemistry, University of California, San Diego, 9500 Gilman Drive MC0358, La Jolla, California 92093, USA*
[3]*IMEC, Kapeldreef 75, B 3001 Leuven, Belgium*

(Received 5 April 2011; accepted 14 July 2011; published online 1 August 2011)

The direct reaction of trimethylaluminum (TMA) on a Ge(100) surface and the effects of monolayer H_2O pre-dosing were investigated using ultrahigh vacuum techniques, such as scanning tunneling microscopy (STM), scanning tunneling spectroscopy (STS), and x-ray photoelectron spectroscopy (XPS), and density functional theory (DFT). At room temperature (RT), a saturation TMA dose produced 0.8 monolayers (ML) of semi-ordered species on a Ge(100) surface due to the dissociative chemisorption of TMA. STS confirmed the chemisorption of TMA passivated the bandgap states due to dangling bonds. By annealing the TMA-dosed Ge surface, the STM observed coverage of TMA sites decreased to 0.4 ML at 250 °C, and to 0.15 ML at 450 °C. XPS analysis showed that only carbon content was reduced during annealing, while the Al coverage was maintained at 0.15 ML, consistent with the desorption of methyl ($–CH_3$) groups from the TMA adsorbates. Conversely, saturation TMA dosing at RT on the monolayer H_2O pre-dosed Ge(100) surface followed by annealing at 200 °C formed a layer of Ge–O–Al bonds with an Al coverage a factor of two greater than the TMA only dosed Ge(100), consistent with Ge–OH activation of TMA chemisorption and Ge–H blocking of CH_3 chemisorption. The DFT shows that the reaction of TMA has lower activation energy and is more exothermic on Ge–OH than Ge–H sites. It is proposed that the H_2O pre-dosing enhances the concentration of adsorbed Al and forms thermally stable Ge–O–Al bonds along the Ge dimer row which could serve as a nearly ideal atomic layer deposition nucleation layer on Ge(100) surface. [doi:10.1063/1.3621672]

I. INTRODUCTION

As the complementary metal-oxide-semiconductor devices scale down, a new material with high carrier mobility may be required to substitute for the conventional silicon channel. Germanium is one of the candidates for the new channel material because it has superior electronic properties (higher hole and electron mobility) compared to silicon. However, a high interface trap density between Ge and Ge native oxide has been a challenge in fabricating Ge-channel MOSFET devices even with high-k gate oxide materials, since GeO_x is often incorporated as an interfacial layer.[1,2]

To minimize the defect density at the interface of a Ge substrate and a gate dielectric layer, a proper passivation is required for a Ge surface prior to the oxide deposition. Various passivation methods have been investigated including epitaxial growth of Si,[3,4] halogenation,[5–7] sulfurization,[8,9] nitridation,[10–12] and oxidation.[13–17] The lowest interface trap densities have been obtained using a stoichiometric GeO_2 layer typically formed by ozone[15] or high pressure oxidation[16] of a Ge substrate. However, for scaling of equivalent oxide thickness, the thickness of this passivation layer has to be minimized – ideally to a monolayer (ML), which is very difficult using GeO_2 because of its thermodynamic instability on bulk Ge ($Ge + GeO_2 \rightarrow 2GeO$).[18]

Swaminathan *et al.* recently reported that the interface quality of a Ge MOS stack was improved when H_2O was pre-pulsed multiple times on a Ge substrate prior to the atomic layer deposition (ALD) of Al_2O_3.[19] Since the activation of trimethylaluminum (TMA) chemisorption was attributed to the formation of Ge–OH bonds, it is likely that one can use H_2O as an alternative oxygen precursor to form an ultrathin passivation layer at relatively low temperature (below 300 °C) thereby minimizing suboxide formation.[18] Moreover, in a separate study, H_2O was shown to provide a well-ordered chemisorption monolayer even at room temperature (RT), without disrupting the surface Ge atoms.[20,21] Therefore, reaction of a Ge surface first with H_2O followed by reaction with a metal precursor (e.g., TMA) at RT is expected to provide an ideal monolayer passivation and ALD nucleation on a Ge surface.

To design a process for a scalable passivation layer using H_2O and metal precursors, it is crucial to understand the reactions of both H_2O and a metal precursor with a Ge surface. Since TMA is the most commonly used metal precursor, there have been numerous studies on the ALD reaction of

a)Author to whom correspondence should be addressed. Electronic mail: akummel@ucsd.edu.

TMA and H_2O on semiconductor surfaces.[22] However, most of the studies were focused on Si surfaces and less is known about the TMA/H_2O reaction with Ge or III-V compound materials.[19,23,24] In addition, the direct reaction of TMA with Si or Ge has not been previously studied since it requires clean (oxygen-free and carbon-free) semiconductor surfaces in a water-free ALD reaction chamber. An extremely clean semiconductor surface can be formed in ultrahigh vacuum (UHV) conditions providing a unique opportunity to study the reactions of H_2O and TMA on a semiconductor surface in a slow, step-wise fashion, while a typical ALD process is performed at 0.1∼100 Torr but with very fast processing.

In this study, the reaction of TMA on a Ge(100) surface and the effect of H_2O pre-dosing were investigated at an atomic level utilizing UHV experimental techniques. The direct reaction of TMA was performed at RT, and the thermal behavior of the reacted surface was studied by annealing at different temperatures in a UHV chamber. The topographic and electronic structures were analyzed *in situ* by scanning tunneling microscopy (STM) and scanning tunneling spectroscopy (STS) while the relative ratio of surface elements was measured using x-ray photoelectron spectroscopy (XPS). To determine the effect of H_2O monolayer functionalization of Ge(100), TMA dosing was also studied on the H_2O predosed Ge(100) surface, and the surface bonding structures were investigated using STM and XPS. Computational analysis on the reaction of TMA on a Ge surface with –OH and –H was performed using calculations based on density functional theory (DFT).

II. METHODS

A. Experimental details

A Sb-doped *n*-type Ge wafer (0.005–0.020 Ωcm, Wafer World Inc.) was cut into rectangular pieces (12.5 mm × 4.5 mm) and degreased via ultrasonication with acetone, methanol, and deionized water followed by drying with N_2 gas. Each Ge sample was introduced into an UHV chamber at a base pressure of 2×10^{-10} Torr and cleaned using several cycles of sputter-anneal to remove the native oxides. The sputtering of each sample was performed using a 2 keV of Ar^+ ion beam (Model 1403 ion gun, Nonsequitur Technologies) with the beam current of 1.4 μA and at an incident angle of 45° for 30 min. During the sputtering process, the sample temperature was maintained at 500 °C using direct heating to avoid the incorporation of trace oxygen on a Ge surface.[18] After each sputtering process, the sample was annealed at 700 °C for 20 min at a base pressure of the main chamber (2×10^{-10} Torr).

The sample was transferred into the separate "dosing" chamber at a base pressure of 5×10^{-9} Torr to dose precursors on the surface. TMA and H_2O dosing was performed by back filling the dosing chamber with the vapor of precursors using their own vapor pressures. The TMA vapor (Strem Chemicals, Inc.) was introduced directly onto the sample surface at RT by throttling the valves on the TMA dosing line and the container. The pressure of TMA was measured using an ion gauge, and the exposure of TMA was estimated in Langmuirs (1 Langmuir (L) = 1×10^{-6} Torr · 1 s). The high-performance liquid chromatography grade H_2O (Fisher Scientific) dose was also performed at RT in the same dosing chamber, but through a different dosing line, by controlling the flow of the H_2O vapor using a needle valve. The dosing chamber was baked out at 150 °C for several hours before and after replacing the dosing source, in order to avoid the cross-contamination between TMA and H_2O.

After each TMA or H_2O dose, the sample was transferred back to the main chamber for a thermal annealing at the base pressure (2×10^{-10} Torr). The ramp rate for the direct heating was controlled at 1 °C/s, while the sample temperature was monitored by a pyrometer.

The *in situ* analysis of the topography of the sample was performed using a STM (LT-STM, Omicron Nanotechnology). The filled-state STM images were obtained using the constant-current mode STM (I_{sp} = 0.2 nA) and applying a sample bias of −1.8 V. The electronic structure of the surface species was measured by STS with a variable-z method using a modulation signal (0.1 V, 650 Hz) from an external lock-in amplifier, while sweeping the sample bias from −1.5 to +1.5 V. All the STM and STS data were obtained at RT at a base pressure of 4×10^{-11} Torr, after the various treatments were employed on the sample. The coverage of surface species after each step of surface treatments was estimated by differentiating the height distribution histogram of the STM image using the STM image processing software (SPIP v4.5.1).

The *in situ* monochromatic XPS (XM 1000 MkII/SPHERA, Omicron Nanotechnology) was used to examine the surface elements and the ratio of their relative intensities. The XPS was operated in a constant analyzer energy mode with the pass energy of 50 eV and the line width of 0.1 eV, using an Al Kα source (1486.7 eV). The takeoff angle was 30° from the sample surface with an acceptance angle of ±7°. The peak analysis process, such as background subtraction and peak fitting, was performed using CASAXPS v2.3. The signal obtained from a clean Ge surface was employed for the background subtraction. The relative XPS intensity of each core-level spectra (C 1*s*, Al 2*p*, and O 1*s*) was quantified by calculating the peak area divided by the XPS sensitivity factor.

B. Computational details

The DFT modeling was employed to investigate the reaction pathways of TMA on the H_2O treated Ge surface. The OH and H surface sites, obtained after dissociative adsorption of H_2O on the Ge dimmers, are represented by two separate clusters $Ge(OH)(GeH_3)_3$ and $Ge(H)(GeH_3)_3$. The DFT calculations of the clusters and their interactions with TMA were performed using the B3LYP gradient corrected hybrid functional and the def2-TZVP basis sets.[25] Geometry optimizations were performed to locate the stationary points. Frequency analyses were performed to check the nature of the structures (e.g., minimum or transition state) and to calculate the zero-point energy corrections. The transition state structures reported below all represent saddle points, characterized by one negative eigenvalue in the Hessian matrix. All

calculations were performed with the PCGAMESS code.[26,27] Reactions including radicals were not calculated due to intrinsic limitations of the DFT.

Rather large clusters are required to adequately describe the structures and reactions occurring on semiconductor substrates.[28,29] However, small clusters including only one surface site give a relevant representation of the local reactivity of a single surface site.[30] They can, therefore, be used to compare the reactivity of a precursor with different functional sites, e.g., Ge–OH versus Ge–H in the present study, while allowing computational hybrid functionals to be employed to calculate accurate activation barriers.

III. RESULTS AND DISCUSSION

A Ge(100) sample was dosed to near saturation at RT with TMA. Figure 1 shows STM and STS results obtained on a Ge(100) surface directly reacted with 10 000 L of TMA. Bright semi-ordered features were observed covering 0.75 ML of the surface in the filled state STM image (green box in Fig. 1(a)). The vertical rows of the semi-ordered structures are aligned parallel with the vertical rows of surface Ge dimers, which are observed through pinholes (blue box in Fig. 1(a)). Examination of the TMA reacted areas reveals that many of the bright sites appear as paired dots with 4 ∼ 5 Å of spacing. The semi-ordered structure is likely consistent with the dissociative chemisorption of the TMA molecules into a dimethylaluminum (DMA) and a methyl group (–CH_3) as shown in the schematic diagram in a green box of Fig. 1(a). The detailed modeling studies are presented later in this paper.

To investigate the electronic structure of the ordered bright sites, STS measurements were performed on bare Ge sites and bright-ordered sites (Fig. 1(b)). It was found that the density of states near 0.7 eV is significantly reduced on the bright sites. The STS is consistent with the dangling bonds on the bare Ge dimers being terminated by the chemisorption of DMA and a methyl group, thereby removing the dangling bond states. Similar phenomena were observed on the H_2O chemisorption sites on a H_2O dosed Ge(100) surface.[21] This is also consistent with the bright-ordered sites in Fig. 1(a) being TMA reaction products which terminate surface dangling bonds and partially passivate the surface. To completely passivate the Ge surface using the TMA chemisorption, the nucleation density of the TMA needs to be increased closer to unity.

The thermal behavior of a TMA chemisorption site was examined by annealing a TMA dosed surface in ultrahigh vacuum (below 2×10^{-10} Torr). Filled-state STM images in Fig. 2 show a Ge(100) surface dosed with 20 000 L of TMA at RT and annealed at 250 °C and 450 °C. A significant decrease in coverage of bright features (from 0.8 ML on as-dosed surface to 0.15 ML on 450 °C annealed surface) is observed in the STM images obtained as a function of the annealing temperature. Schematic diagrams of possible surface structures are also shown on the right side of each STM image. For an as-dosed Ge surface, the dissociative chemisorption and the coordinative bonding of TMA are proposed (case a1 and a2 in Fig. 2(a)). The chemisorption of TMA (case a1) is consistent with passivating the surface dangling bonds even with a low Al coverage since at least one methyl group bonds to the Ge surface. The coordinative or dative bond of TMA (case a2) possibly occurs with the electron pair donated from an up-Ge dimer atom.[22,31,32] However, dative bonding is likely to be unstable for long periods in ultrahigh vacuum; case a1 is also consistent with the known stability of –CH_3 on Ge(100) at RT.[33] Therefore, case a1 is hypothesized to be the structure for TMA reaction at RT.

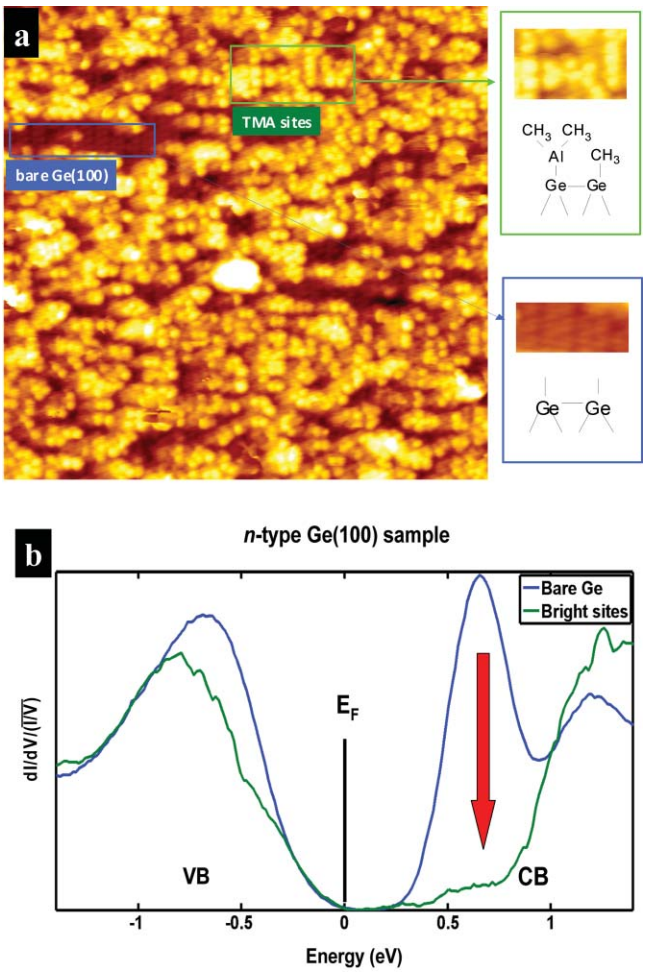

FIG. 1. STM and STS obtained from a Ge(100) surface dosed with 10 000 L of TMA at RT. (a) Filled state STM image (Vs = −1.8 V, It = 0.2 nA, 30 nm × 30 nm) indicates semi-ordered TMA chemisorption sites (green box) and bare Ge(100) sites through pinholes (blue box). Corresponding zoom-in images and schematic diagrams are shown on the right. (b) STS curve measured on bright TMA sites (green) shows a significant reduction of the dangling bond states near 0.7 eV (red arrow) compared to the STS curve measured on bare Ge sites (blue).

On a 250 °C annealed surface, the TMA-derived species with a diameter ranging from 4∼8 Å cover 0.4 ML of the surface; three different structures are considered for these species (Fig. 2(b)). Recombination of two methyl groups results in monomethylaluminum (MMA; case b1) with C_2H_6 as a byproduct, while recombinative desorption between H and –CH_3 result in surface structures shown in the diagrams of cases b2 and b3 in Fig. 2(b) with CH_4 as a byproduct. Since cases b1 and b2 are likely to be ∼9.6 kcal/mol more exothermic than b3 based on polyatomic bond strengths[34–36]

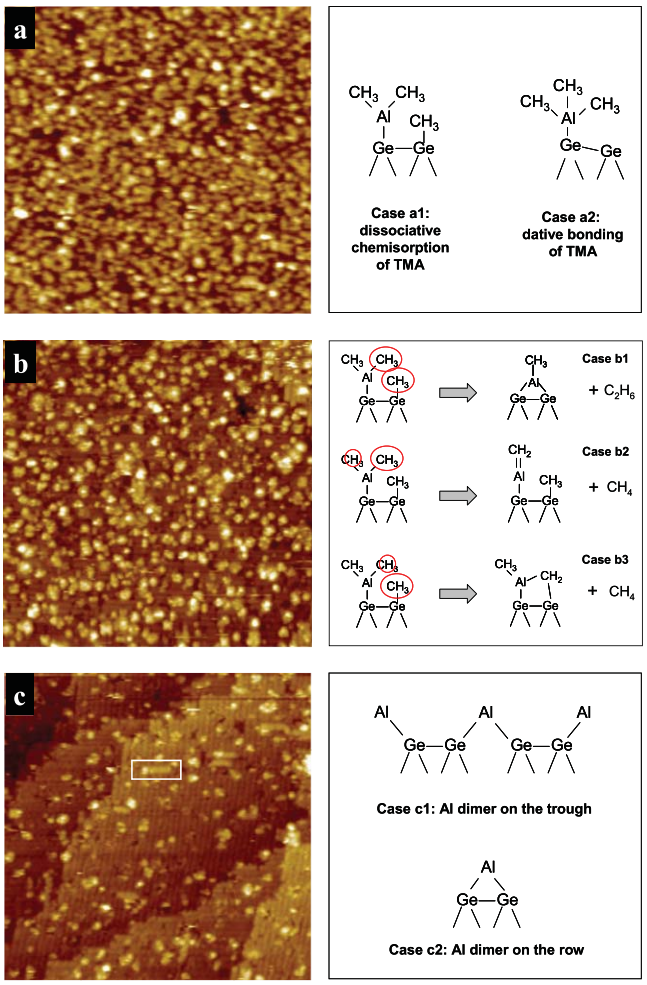

FIG. 2. STM images (Vs = −1.8 V, It = 0.2 nA, 50 nm × 50 nm) of a Ge(100) surface dosed with 20 000 L of TMA followed by no anneal (a), annealing at 250 °C (b), and annealing at 450 °C (c). The possible structures corresponding to each surface are shown on the right. (a) As-dosed surface at RT is covered by 0.8 ML of bright TMA sites. (b) The 250 °C annealed surface shows TMA-derived species covering 0.4 ML of surface. (c) The 450 °C annealed surface still has TMA-derived species but with less coverage (0.15 ML). Bright features perpendicular to the Ge dimer rows are observed in the white box (possible Al dimer rows). It is noted that XPS still shows a Al:C ratio of 1:1 after a 450 °C (see Fig. 3(a)) and the 450 °C annealed surface shows structures similar to the ones on the 250 °C annealed surface indicating presence of residual DMA or MMA; therefore, it is possible that many of structures on the 450 °C annealed surface are DMA or MMA.

(described in Fig. 5(a)), b1 and b2 are considered to be the most likely structure at 250 °C.

The TMA-derived species observed on 250 °C annealed surface still remain on a 450 °C annealed surface, covering ∼0.15 ML of the surface (Fig. 2(c)). In addition, bright rows perpendicular to the background Ge dimer rows are occasionally observed as shown in the white box in Fig. 2(c). Since similar features were observed on a Si(100) surface with thermal evaporation of pure Al (Ref. 37) and with direct dosing of dimethylaluminum hydride (DMAH) at 700 K,[38] the structure in the white box is assumed to be Al dimer rows. It is likely that the residual methyl groups dissociate from Al at 450 °C, leaving elemental Al features on the surface and initiating the formation of bare Al dimers. Two different cases of the Al dimer row are shown in the diagram of Fig. 2(c); Al dimer on the trough (case c1) and Al dimer on the row (case c2). In both structures, Al is dimerized with another Al atom behind obscured for the perspective of the diagram. Since case c1 has less bond angle strain assuming tetrahedral bonding for Ge, it is hypothesized to be the more likely structure. It is noted that XPS still shows a Al:C ratio of 1:1 after annealing at 450 °C (see below) and the 450 °C annealed surface shows structures similar to the ones on the 250 °C annealed surface indicating presence of residual DMA or MMA; therefore, it is possible that many of the features shown in Fig. 2(c) are DMA or MMA.

To examine the chemical composition of the surface, XPS measurement was performed on the Ge(100) surface with various treatments. The binding energies of the XPS spectra from each core-level showed a good agreement with standard values.[39] However, it was difficult to detect the chemical shift of the Ge 3*d* core-level corresponding to various oxidation states probably due to a submonolayer coverage of Ge oxide.[40] Furthermore, the XPS spectra from the surface elements (C, O, Al) showed poor signal to noise ratio which made it challenging to analyze the chemical environment of these submonolayer elements. However, the relative XPS intensities of surface elements showed consistent ratios between several experiments. Consequently, a reasonable estimation of surface coverage of each element could be derived by quantifying the relative XPS intensities using the peak areas and sensitivity factors.

Figure 3(a) shows the estimated coverage of surface elements from XPS intensities calibrated to the Ge 3*d* feature intensity. With a saturation dose of TMA on Ge(100) at RT, the ratio of C:Al was about 2.8:1. By annealing up to 450 °C, the carbon content decreases while the Al content remains almost constant, resulting in the ratio of C:Al as 1.2:1. This is consistent with desorption of methyl or methyl-related byproducts during the thermal annealing as described in Fig. 2. The carbon remaining on the 450 °C annealed surface is attributed to the residual DMA or MMA species due to the insufficient annealing time (5 min), which is consistent with the TMA-derived species observed on a STM image of a 450 °C annealed surface (Fig. 2(c)).

The Al coverage being independent of annealing temperature indicates the coverage of surface species at 450 °C observed by STM (0.15 ML) being the maximum or nominal coverage of Al for a saturation dose of TMA at RT. It is hypothesized that the steric hindrance of methyl ligands and the chemisorption of methyl groups on Ge surface restrict the nucleation density of Al via the direct reaction of TMA on Ge(100) at RT.

To investigate the effect of H_2O chemisorption on TMA nucleation, XPS measurements were performed on the Ge surface pre-dosed with 1×10^6 L of H_2O, followed by 60 000 L TMA dose at RT (Fig. 3(b)). The ratio of O:C:Al was 1.2:2.7:1. Similar to the case of TMA dosed surface, the C content decreased as the annealing temperature increased, while the Al content remained constant. However, the Al coverage for the TMA+H_2O dosed Ge surface was about a factor of two greater than the Al coverage for the TMA only dosed Ge surface. Furthermore, the ratio of O:Al was invariant with annealing temperature up to 450 °C. This is consistent with

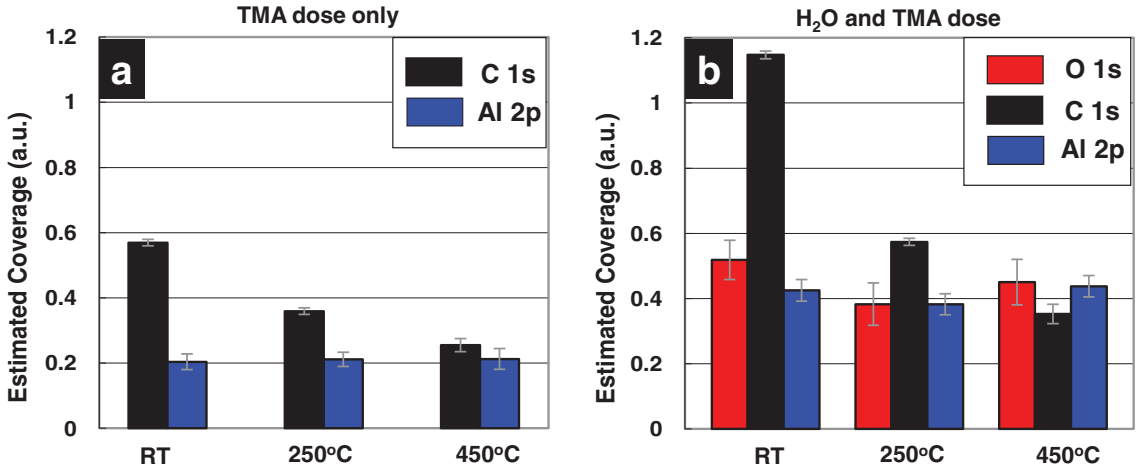

FIG. 3. Coverage of surface elements estimated from relative XPS intensities. XPS sensitivity for each core-level spectra was taken into account to compare intensities from different elements. All the data presented are derived from the ratios to the Ge3*d* feature intensity. Error bars (standard deviations) are shown on the histograms. (a) On a saturation TMA dosed Ge(100) at RT, C:Al ratio is 2.8:1. By annealing to 450 °C, only C content decreases while Al amount remains the same. (b) A saturation dose of H_2O followed by TMA at RT produces 1.2:2.7:1 of O:C:Al ratio. By annealing up to 450 °C, only C content decreases while O and Al intensities remain the same. Note that the amount of Al increased as a factor of two on the H_2O pre-dosed Ge(100) surface.

TMA readily bonding on hydroxyl sites at RT, forming thermally stable Al–O–Ge bonds. Since a $–CH_3$ dissociated from TMA can recombine with a hydrogen atom when TMA bonds on –OH (the well-documented ligand exchange reaction[22]), the steric hindrance of the TMA ligands and the methyl site blocking issues could be reduced compared to the TMA only case. As noted below in the DFT calculation (see below), the ratio of C/Al at RT prior to annealing being greater than two is consistent with the formation of coordinative complex of TMA, the dissociation of TMA on Ge–OH being thermally activated, and the existence of a stable molecular chemisorption site at RT.

To verify the bonding structures of the surface, STM measurements were performed on a Ge surface pre-dosed with 7×10^5 L H_2O followed by 35 000 L dosing of TMA at RT (Fig. 4). Although a poor H_2O dose left a high density of bright dangling bond sites, semi-ordered regions are observed on the surface after annealing at 200 °C as shown in the white box in the STM image of Fig. 4. Line profile analysis shows the vertical rows which have 8∼9 Å of spacing. Considering

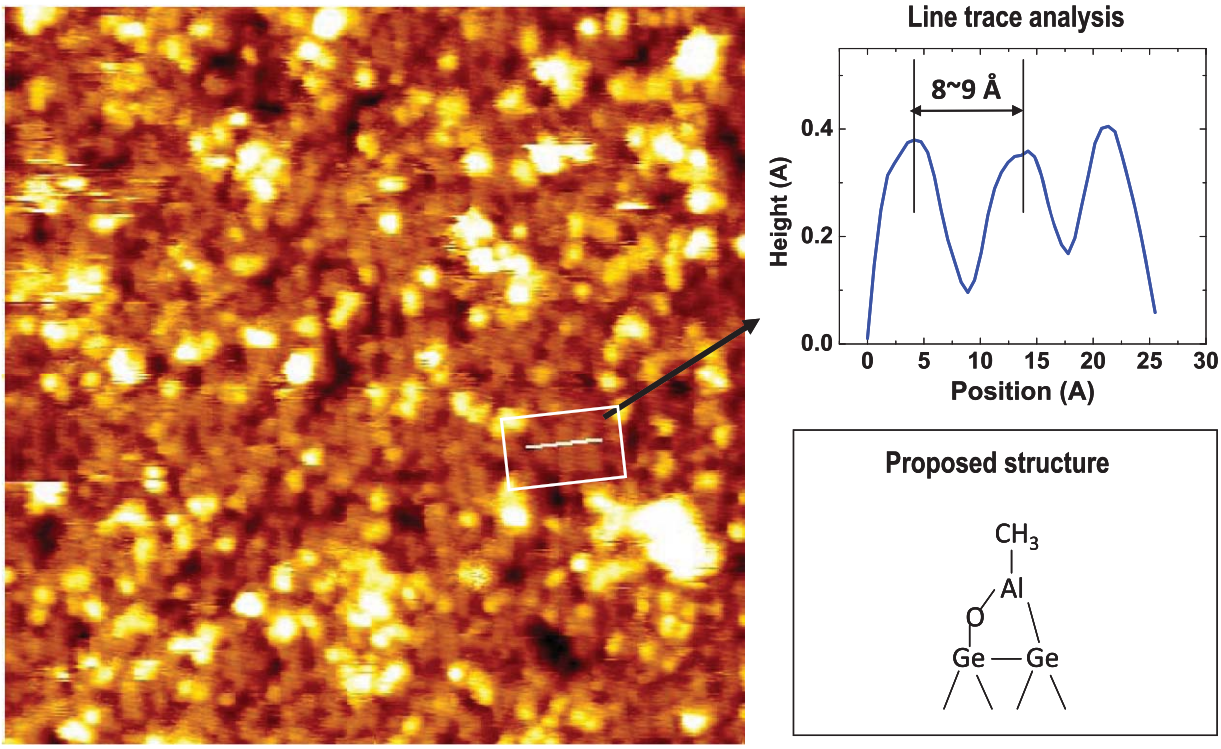

FIG. 4. Filled state STM image (30 nm × 30 nm) of 7×10^5 L H_2O dosed Ge(100) followed by 35 000 L TMA dosing at RT and annealing at 200 °C. An ordered structure is observed (white box). Line profile shows the spacing of vertical rows is ∼9 Å and proposed structure is shown on the bottom right.

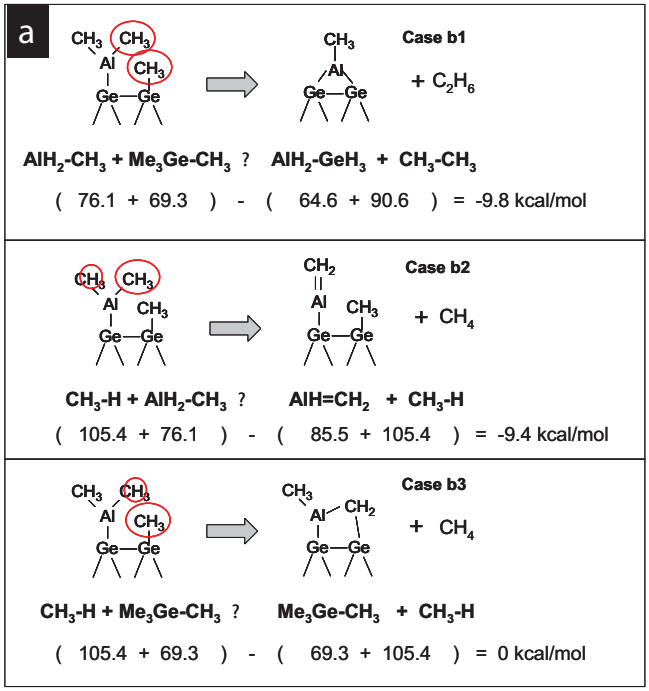

c

Bond	Energy (kcal/mol)
Me_3Ge-CH_3	69.3[α]
AlH_2-CH_3	76.1[β]
AlH=CH_2	85.5[β]
AlH_2-SiH_3	64.6[β]
AlH_2-GeH_3	64.6*
CH_3-H	105.4[α]
CH_3-CH_3	90.6[α]
Me_3Ge-H	81.6[γ]

α: ref 34, β: ref 35, γ: ref 36, *: inferred from AlH_2-SiH_3

FIG. 5. Estimation of exothermicity using polyatomic bond strengths. (a) Exothermicity of proposed reactions of TMA on a Ge(100) surface at 250 °C (Fig. 2(b)). (b) Exothermicity of proposed reaction of TMA on a H_2O dosed Ge surface at 250 °C (Fig. 4). (c) Table of polyatomic bond energies.

the symmetry of the bonding structure and the elemental ratio obtained from XPS, a model structure is proposed in the bottom of Fig. 4. Since the H_2O dosed Ge surface has one –OH and one –H on each dimer, it is plausible that an Al atom on a Ge dimer will eventually make two bonds; one on a Ge atom directly and the other on O atom atop of Ge with the estimated exothermicity of –12.3 kcal/mol (Fig. 5(b)) or –10.8 kcal/mol (as estimated by the more accurate DFT calculations below).

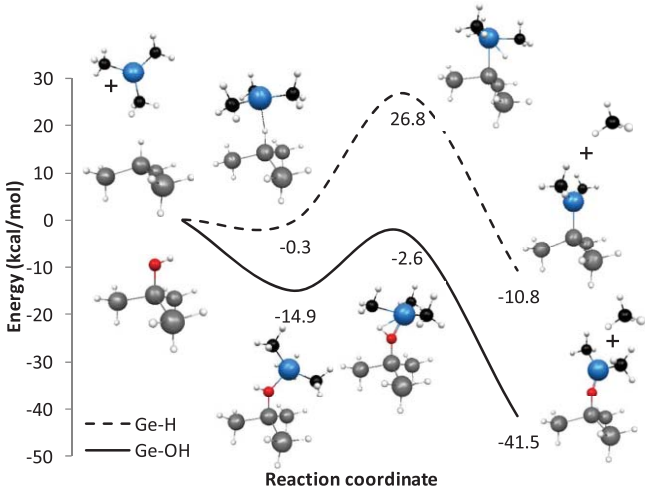

FIG. 6. Potential energy of surfaces calculated for the adsorption of TMA on –Ge–OH and –Ge–H. The stable and transition state structures for the TMA reactions are indicated. In these structures, the Ge atoms are displayed in grey, H in white, Al in blue, and O in red. The energies in kcal/mol were calculated relative to the energy of the reagents.

Further analysis of STM and STS were not available due to the extremely unstable tunneling signal from the surface indicating the formation of ultrathin AlO_x layer.

The reactivity of –Ge–OH and –Ge–H sites for TMA adsorption were compared using DFT calculations. The following reactions of TMA were considered:

$$Al(CH_3)_3 + (GeH_3)GeOH \rightarrow (GeH_3)GeOAl(CH_3)_2 + CH_4,$$

$$Al(CH_3)_3 + (GeH_3)GeH \rightarrow (GeH_3)GeAl(CH_3)_2 + CH_4.$$

The potential energy surfaces for the TMA reaction with –Ge–OH and –Ge–H are shown in Fig. 6. The reaction of TMA with –Ge–OH proceeds by a similar pathway as with –Al–OH.[30,41] First, a coordinative complex forms through electron donation of O to Al. The binding energy of the complex is –14.9 kcal/mol, consistent with XPS results showing a C:Al ratio of 2.7:1 at RT. The strong coordinative bond results in a tetrahedral Al coordination environment: the C–Al–C bond angle decreases from 120° to 115.1°. Conversely, the complex of TMA with –Ge–H is weak and the calculated binding energy is negligible (–0.3 kcal/mol). The Al–H bond distance is long (2.21 Å) and the Al coordination with the three CH_3 groups remains almost planar as indicated by the C–Al–C bond angles of 119.3°.

In the transition state, the Al–O or Al–Ge bond distances decrease (for reaction with –Ge–OH or –Ge–H, respectively) and a hydrogen atom is transferred to one of the $–CH_3$ groups of TMA to form CH_4 as a reaction product. Due to an additional Al–H interaction, the Al atom is pentacoordinated in the transition state, while after the reaction, the Al coordination again becomes threefold and planar. The energy barrier as compared to the energy of the coordinative complexes is much higher for reaction with –Ge–H (27.1 kcal/mol) than with –Ge–OH (12.3 kcal/mol). In the case of reaction with –Ge–OH, the energy of the transition state structure is even

slightly lower than the initial reagents. The TMA reaction will, therefore, proceed with slower kinetics on the –Ge–H site as compared to –Ge–OH site. Both reactions are favorable from a thermodynamic point of view, but the exothermicity is much larger for –Ge–OH (–41.4 kcal/mol) as compared to –Ge–H (−10.8 kcal/mol).

Combining experimental and theoretical results, it is hypothesized that at RT, TMA adsorbs on the –GeOH site of the Ge dimer and not on the –GeH site, consistent with the XPS data showing O:Al ratio of 1.2:1 in Fig. 3(b). The XPS furthermore indicates that the TMA reaction at RT mainly forms the coordinative complex but some adsorbed TMA molecules react further with –Ge–OH to form DMA, resulting in the slight reduction of carbon. This is consistent with the C:Al ratio of 2.7:1 in Fig. 3(b). By annealing at 250 °C, the C:Al ratio decreases to 1.5:1, indicating the further conversion to DMA through the reaction with –Ge–OH or even to MMA as shown in XPS (Fig. 5(b)) and STM (Fig. 4) observation. The formation of MMA occurs further at high annealing temperature (450 °C), consistent with the reduction of carbon in XPS (Fig. 5(b)). This could occur by much slower reaction of the DMA fragment with a neighboring –GeH site or by other reaction mechanisms, e.g., involving radicals.

IV. CONCLUSIONS

Direct reaction of TMA on a Ge(100) surface at RT was investigated at an atomic level, and the thermal behavior of surface species was examined. It is found the TMA chemisorption on clean Ge(100) partially passivates the Ge(100) surface by terminating the surface dangling bonds, but the nucleation density of Al is restricted due to the steric hindrance and substantial adsorption of methyl groups. Poor nucleation density of Al in the direct reaction of TMA on Ge(100) suggests that the oxidant-first ALD initiation is needed to obtain pinhole-free nanoscale oxide growth via ALD on the Ge(100) surface. Functionalization of Ge(100) with a monolayer of H_2O enhances the nucleation of TMA, maintains a flat surface, and provides a thermally stable Al–O bond which offers a high density initiation layer for other high-k materials. The DFT calculations showed that the reaction of TMA is more favorable on the Ge–OH sites than on the Ge–H sites. The combination of monolayer H_2O functionalization followed by a TMA reaction doubles the Al nucleation density which may be critical to prevent pinhole formation in the aggressive scaling of gate oxide thickness.

ACKNOWLEDGMENTS

This work is supported by the MSD Focus Center Research Program (2051.001). The authors would like to acknowledge Prof. Wallace group at UT Dallas for their helpful discussions on the XPS experiments. The authors would also like to acknowledge Prof. K. Pierloot from the University of Leuven for helpful discussions regarding the DFT calculations.

[1] Y. Kamata, Mater. Today **11**(1–2), 30 (2008).
[2] M. Caymax, M. Houssa, G. Pourtois, F. Bellenger, K. Martens, A. Delabie, and S. VanElshocht, Appl. Surf. Sci. **254**(19), 6094 (2008).
[3] B. DeJaeger, R. Bonzom, F. Leys, O. Richard, J. V. Steenbergen, G. Winderickx, E. V. Moorhem, G. Raskin, F. Letertre, T. Billon, M. Meuris, and M. Heyns, Microelectron. Eng. **80**, 26 (2005).
[4] N. Taoka, M. Harada, Y. Yamashita, T. Yamamoto, N. Sugiyama, and S.-I. Takagi, Appl. Phys. Lett. **92**(11), 113511 (2008).
[5] P. Ardalan, E. R. Pickett, J. S. Harris, Jr., A. F. Marshall, and S. F. Bent, Appl. Phys. Lett. **92**(25), 252902 (2008).
[6] S. Sun, Y. Sun, Z. Liu, D.-I. Lee, and P. Pianetta, Appl. Phys. Lett. **89**(23), 231925 (2006).
[7] R. Xie, M. Yu, M. Y. Lai, L. Chan, and C. Zhu, Appl. Phys. Lett. **92**(16), 163505 (2008).
[8] T. Maeda, S. Takagi, T. Ohnishi, and M. Lippmaa, Mater. Sci. Semicond. Process. **9**, 706 (2006).
[9] R. Xie and C. Zhu, IEEE Electron Device Lett. **28**, 976 (2007).
[10] H. Kim, P. C. McIntyre, C.-O. Chui, K. C. Saraswat, and M.-H. Cho, Appl. Phys. Lett. **85**(14), 2902 (2004).
[11] T. Maeda, T. Yasuda, M. Nishizawa, N. Miyata, Y. Morita, and S. Takagi, J. Appl. Phys. **100**(1), 014101 (2006).
[12] T. Sugawara, R. Sreenivasan, and P. C. McIntyre, J. Vac. Sci. Technol. B **24**(5), 2442 (2006).
[13] F. Bellenger, M. Houssa, A. Delabie, V. Afanasiev, T. Conard, M. Caymax, M. Meuris, K. DeMeyer, and M. M. Heyns, J. Electrochem. Soc. **155**(2), G33 (2008).
[14] A. Delabie, F. Bellenger, M. Houssa, T. Conard, S. VanElshocht, M. Caymax, M. Heyns, and M. Meuris, Appl. Phys. Lett. **91**(8), 082904 (2007).
[15] D. Kuzum, T. Krishnamohan, A. J. Pethe, A. K. Okyay, Y. Oshima, Y. Sun, J. P. McVittie, P. A. Pianetta, P. C. McIntyre, and K. C. Saraswat, IEEE Electron Device Lett. **29**(4), 328 (2008).
[16] C. H. Lee, T. Tabata, T. Nishimura, K. Nagashio, K. Kita, and A. Toriumi, ECS Trans. **19**(1), 165 (2009).
[17] H. Matsubara, T. Sasada, M. Takenaka, and S. Takagi, Appl. Phys. Lett. **93**(3), 032104 (2008).
[18] K. Prabhakaran, F. Maeda, Y. Watanabe, and T. Ogino, Thin Solid Films **369**(1–2), 289 (2000).
[19] S. Swaminathan, Y. Oshima, M. A. Kelly, and P. C. McIntyre, Appl. Phys. Lett. **95**(3), 032907 (2009).
[20] J. S. Lee, S. R. Bishop, T. Kaufman-Osborn, E. Chagarov, and A. C. Kummel, ECS Trans. **33**(6), 447 (2010).
[21] J. S. Lee, T. Kaufman-Osborn, W. Melitz, S. Lee, and A. Kummel, Surf. Sci. **605**(15–16), 1583 (2011).
[22] R. Puurunen, J. Appl. Phys. **97**(12), 121301 (2005).
[23] J. B. Clemens, E. A. Chagarov, M. Holland, R. Droopad, J. Shen, and A. C. Kummel, J. Chem. Phys. **133**(15), 154704 (2010).
[24] M. Milojevic, R. Contreras-Guerrero, M. Lopez-Lopez, J. Kim, and R. M. Wallace, Appl. Phys. Lett. **95**(21), 212902 (2009).
[25] F. Weigend and R. Ahlrichs, Phys. Chem. Chem. Phys. **7**, 3297 (2005).
[26] A. Granovsky, Firefly version 7.1.G, see http://classic.chem.msu.su/gran/firefly/index.html.
[27] W. Schmidt, K. K. Baldridge, J. A. Boatz, S. T. Elbert, M. S. Gordon, J. H. Jensen, S. Koseki, N. Matsunaga, K. A. Nguyen, S. Su, T. L. Windus, M. Dupuis, and J. A. Montgomery, J. Comput. Chem. **14**, 1347 (1993).
[28] M. D. Halls and K. Raghavachari, J. Phys. Chem. A **108**(15), 2982 (2004).
[29] Y. Widjaja and C. B. Musgrave, Surf. Sci. **469**(1), 9 (2000).
[30] Y. Widjaja and C. Musgrave, Appl. Phys. Lett. **80**, 3304 (2002).
[31] M. A. Filler and S. F. Bent, Prog. Surf. Sci. **73**(1–3), 1 (2003).
[32] X. Cao and R. J. Hamers, J. Phys. Chem. B **106**(8), 1840 (2002).
[33] P. Y. Chuang, W. L. Lee, T. F. Teng, Y. H. Lai, and W. H. Hung, J. Phys. Chem. C **113**(40), 17447 (2009).
[34] *CRC Handbook of Chemistry and Physics*, 91st ed., edited by W. M. Haynes (CRC/Taylor & Francis, Boca Raton, FL, 2010).
[35] P. Schleyer and D. Kost, J. Am. Chem. Soc. **110**(7), 2105 (1988).
[36] A. M. Doncaster and R. Walsh, J. Phys. Chem. **83**(5), 578 (1979).
[37] J. Nogami, A. A. Baski, and C. F. Quate, Phys. Rev. B **44**(3), 1415 (1991).
[38] T. Mitsui, E. Hill, R. Curtis, and E. Ganz, Phys. Rev. B **59**(12), 8123 (1999).
[39] See supplementary material at http://dx.doi.org/10.1063/1.3621672 for estimation of exothermicity.
[40] D. Schmeisser, R. D. Schnell, A. Bogen, F. J. Himpsel, D. Rieger, G. Landgren, and J. F. Morar, Surf. Sci. **172**(2), 455 (1986).
[41] L. Nyns, A. Delabie, G. Pourtois, S. V. Elshocht, C. Vinckier, and S. D. Gendt, J. Electrochem. Soc. **157**, G7 (2010).